

CHARACTERISTICS OF AN ENERGY AND TIME ANALYSIS SYSTEM  
USING A Ge(Li) AND A FAST SCINTILLATION DETECTORS

H. ABOU-LEILA, S. M. DARWISH<sup>1)</sup>, H. A. ISMAIL<sup>2)</sup>, M. KAMEL<sup>2)</sup>

S. EL MENYAWI AND H. EL SAMMAN

Physics Department, University College for Girls,  
Ein Shams University, Cairo, Egypt.

Abstract

The characteristics, performances and capabilities of a system which can measure energies, intensities and lifetimes of gamma transitions in radioactive nuclei using a relatively large volume 76.1 cc Ge(Li) detector and a fast scintillation detector, was discussed. The system was used to measure the half-life of the 482 keV level in  $^{181}\text{Ta}$  nucleus and was found to be  $10.49 \pm 0.09$  ns. The obtained experimental transition probabilities of the different gamma transitions depopulating this level were compared with the theoretical estimates of the single particle model.

---

1) Physics Department, Faculty of Science, Cairo University, Giza, Egypt.

2) Physics Department, Faculty of Education, Ein Shams University, Egypt.

## 1. Introduction

Scintillation detectors are still the fastest nuclear radiation detectors suitable for timing experiments. However, the excellent energy resolution of Ge(Li) detectors compared with scintillation detectors have encouraged many extensive<sup>1-8)</sup> work to study the timing properties of relatively small volume detectors ( $\leq 50$  cc). Such extensive work concerning the timing properties of relatively high volume Ge(Li) detectors ( $\geq 50$  cc) does not exist. In other words, the comparison of calculated time distribution with experimental time spectra<sup>9-13)</sup> have not given complete agreement. In addition, relatively large high volume Ge(Li) detectors have better detection efficiency and thus they are more suitable for low activity measurements and detection of high energy gamma-rays.

The aim of this work is to investigate the characteristics, performances and capabilities of a system which can measure energies, intensities and lifetimes of gamma transitions in radioactive nuclei using a relatively large volume Ge(Li) detector (76.1 cc) and a fast scintillation detector. This system (together with a gamma-gamma coincidence system described before<sup>14)</sup>) is a part of a project in which the decay schemes of some radioactive nuclei will be studied<sup>15)</sup>. However, in this work also, the system was used to measure the half-life of the 482 keV level in  $^{181}\text{Ta}$  nucleus. The obtained experimental transition probabilities of the different gamma transitions depopulating this level were compared with the theoretical estimates of the single particle model<sup>16)</sup>.

## 2. System Description

Fig. 1 shows a block diagram of the system. It consists of three distinct parts :

## 1) DETECTORS

— 103 —

The scintillation detectors constructed for use in this work, consists of a fast XP 1020 Philips photomultiplier tube and a suitable mechanical assembly which permit the housing of different crystals and the necessary electronics. The construction was made to allow the ability of using scintillators whose thicknesses may vary from few mm to about 60 mm. Considering the electronic part, a suitable voltage divider network with decoupling condensers with a chain current of  $1.5 \times 10^{-3}$  amp./ kilovolts and a focus controll was constructed. The fast negative output was taken directly from the anode of the photomultiplier while the linear positive output was taken from the ninth dynode. For this purpose, a low noise preamplifier having an emitter follower stage has been also constructed.

The Ge(Li) detector used was a coaxial ORTEC detector type VIP<sup>10</sup> having a diameter of 4.45 cm and a height of 5.83 cm while its active volume is 76.1 cc. The preamplifier used was also an ORTEC 120B4 charge sensitive preamplifier mounted directly on the detector cryostat so that the input field effect transistor is kept at low temperature in order to provide good stability and low noise level.

## ii) FAST LOGIC CHANNELS

Fast pulses from the anode of the photomultiplier are shaped by a constant fraction discriminator with an amplitude risetime compensation and then fed to the start input of a start-stop time to amplitude converter. Pulses from the timing output of the Ge(Li) detector preamplifier are amplified by a timing filter amplifier to optimize the signal to noise ratio, shaped by a second constant fraction discriminator and then fed to the stop input of the time to amplitude converter through suitable 50- $\Omega$  delay cables. One of the time to amplitude

converter outputs is fed to an Intertechnique 400 channel analyzer for time analysis while the other output is fed to the first input of a triple coincidence circuit through a suitable single channel analyzer and delay.

### iii) SLOW LINEAR CHANNELS

The linear output from the photomultiplier was taken from the ninth dynode while that of the Ge(Li) detector was taken from the energy output of the detector preamplifier. Each of these outputs was amplified and then fed to a timing single channel analyzer. The outputs of these single channel analyzers are fed after suitable delays to the second and third inputs of the triple coincidence circuit whose output gates the multichannel analyzer for timing analysis.

Pulses from the Ge(Li) detector amplifier are fed to a biased amplifier which permit the division of the gamma-ray spectrum into several energy portions and expand each portion to cover the whole memory of a 512-LABEN multichannel analyzer and thus permit energy analysis down to 0.2 keV/channel. Each spectrum was thus recorded in series of overlapping segments. Both the detector amplifier and the biased amplifier were equipped with a base line restorer while a pile up rejector was present in the biased amplifier.

## 3. System Investigation

### 3.1) DETECTORS

#### a) Scintillation Detector :

The detector was found to have an energy resolution 12 % for the 661 keV line of  $^{137}\text{Cs}$  source when using a 50 mm diameter x 50 mm

high NaI(Tl) crystal while the fast anode pulses were found to have a mean risetime  $\approx 3$  ns and a mean width at half maximum 200 ns when using 50 mm dia x 50 mm high NE102 plastic scintillator and a  $^{137}\text{Cs}$  source .

b) Germanium Lithium Detector :

i) Energy Resolution

Although that this detector is of the high resolution type, yet, the best resolution obtained largely depends on the choice of the best working potential as well as the degree of matching and the way of coupling between the electronic equipments processing its signal output. Such conditions are specific for each detector and thus a systematic study of the dependence of the detector resolution on these conditions was performed. Regarding the dependence of the detector noise (preamplifier output) on the applied bias, the noise level at different bias voltages was measured by a 100 Mega cycles Tektronix oscilloscope model 465 after being amplified 40 times by an ORTEC low noise 47Z spectroscopy amplifier (Fig. 2a). At bias voltages greater than 500 volts, the noise level was largely reduced to about 250 microvolts owing to the decrease in the detector capacity. Upon increasing the bias, the detector noise remains nearly constant up to a bias voltage of the order of 3550 volts at which the detector noise began to increase again due to the increase in the leakage current through the detector. Therefore, we can conclude that the best working potential of the detector is  $\approx 3400$  volts at which, the detector has a minimum capacity and negligible leakage current.

However, the effect of the detector bias on the detector pulse height output was also measured using a  $^{137}\text{Cs}$  source (fig. 2b) .

The pulse height output was analyzed on the 512-LABEN multichannel

analyzer and was found to be nearly constant (photo-peak position) over the range from  $\sim 2000$  to  $3500$  volts above which the peak shape began to be distorted.

The energy resolution of the spectrometer (the full width at half maximum of the <sup>photo</sup>/peak) was then measured using a  $^{60}\text{Co}$  source at different shaping time constants of the detector main amplifier ( $0.5, 1, 2, 3$  and  $6 \mu\text{s}$ ). In this investigation, a  $^{60}\text{Co}$  source was put at about  $25$  cm distance from the detector and the integral counting rate was of the order of  $1000$  c/s. From this investigation, (fig. 3) a minimum resolution of  $2.3$  keV for the  $1332$  keV line in  $^{60}\text{Co}$  was obtained for shaping time constant  $\geq 3 \mu\text{s}$ . Since large shaping time constants are not recommended for higher counting rates, a  $3 \mu\text{s}$  shaping time constant was considered to be the most suitable for our detector. At this condition a photopeak to Compton ratio of  $32/1$  was also obtained for the same  $^{60}\text{Co}$  source.

Concerning the way of coupling between the detector main amplifier and the biased amplifier together with the effect of base line restoration in both amplifiers, the best settings to get the best resolution could only be done by experimental empirical means since there are many undefined variables for each particular system. For this reason, the energy resolution of the spectrometer (at  $E_{\gamma} \approx 1332$  keV) was investigated at counting rates ranging from  $\approx 3 \times 10^2$  c/s up to  $\approx 3 \times 10^4$  c/s at three different levels of the discriminator used for base line restoration of the main detector amplifier (low, medium, and high) and at three different input circuit selection modes of the biased amplifier (D. C. coupled, A. C. coupled with low or high base line restoration). Fig. 4 shows the dependence of the spectrometer energy resolution for different settings. It is clear that as long

as the counting rate is  $\leq 5 \times 10^3$  c/s, the base line restorer discriminator set at a medium level and a D. C. coupling between the main amplifier and the biased amplifier seems to be the most suitable settings. However, at counting rates  $> 5 \times 10^3$  c/s, a high setting of the base line discriminator restorer level of the main amplifier and A. C. coupling with high level base line restoration of the biased amplifier are necessary to keep reasonable energy resolution. Otherwise a drastic deterioration of the spectrometer resolution is noticed.

In order to obtain the intrinsic resolution of the detector and the contributions of the electronic noise to the spectrometer resolution, the dependence of the spectrometer resolution on different gamma ray energies ranging from 150 to 2750 keV was studied. In this investigation, we have used the well known gamma-ray transitions in  $^{24}\text{Na}$ ,  $^{131}\text{Ba}$ ,  $^{152}\text{Eu}$ ,  $^{182}\text{Ta}$  and  $^{226}\text{Ra}$  sources. Fig. 5 shows a plot of the linear variations of the spectrometer resolution with the square root of the gamma ray energy. From this figure and using the least square fitting method, the following empirical formula was constructed to express the spectrometer resolution as a function of gamma-ray energy,

$$E \text{ (keV)} = (0.05 \pm 0.002)\sqrt{E} + (0.64 \pm 0.05)$$

From this deduced formula the intrinsic resolution of the detector was found to be  $(0.05 \pm 0.002)\sqrt{E}$ , while the contribution of the electronic noise was  $(0.6 \pm 0.05)$  keV.

Comparing our experimental value of the intrinsic detector resolution to the theoretical value given by <sup>17)</sup>  $2.35\sqrt{\omega F E_{\gamma}}$ , where  $\omega$  is the energy needed to produce one electron hole pair (2.8 eV) and  $F$  is the Fano factor, the Fano factor of our detector was found to be 0.16

#### ii) Detector Photopeak Efficiency

The detector efficiency of the spectrometer by the photoelectric effect varies rapidly with the energy of gamma-rays. However, in most of the experiments in nuclear spectroscopy, only the relative intensities of different gamma transitions emitted by radioactive nuclei are needed. Therefore, only the relative rather than the absolute photopeak detection efficiency of the spectrometer is all that required.

Since the shape of the photopeak efficiency curve of the detector was found to depend on the source to detector distance<sup>18)</sup> and the counting rate<sup>19)</sup>, we have measured the relative photopeak efficiency of our detector at different gamma-ray energies in the energy range from 180 to 2400 keV. Using the well known gamma-ray transition intensities in  $^{131}\text{Ba}$ ,  $^{152}\text{Eu}$ ,  $^{182}\text{Ta}$  and  $^{226}\text{Ra}$  sources at a source to detector distance = 25 cm and at counting rate = 1000 c/s. In this investigation, the gains of both the detector main amplifier and the biased amplifier were adjusted in such a way to be able to expand part of the gamma spectrum on the analyzer to obtain  $\approx 0.5$  keV/channel. The complete spectrum of each source was thus obtained by taking a series of overlapped portions (from 6 to 8 portions) of the spectrum. Each portion was analyzed using the 512 multichannel analyzer and then normalized to each other to obtain the complete spectrum. The relative photopeak efficiency curves obtained for different radioactive sources overlap each other at a certain range of energy and thus could be normalized to each other to obtain the relative photopeak efficiency of the detector as a function of gamma-ray energy as shown in (fig. 6.) Taking into considerations, the statistical errors and the errors involved (average of 4 complete measurements of each spectrum) in

the intensities of the gamma-ray transitions used in this investigation, the errors in determining the values of the relative photopeak efficiency of the detector was found to be of the order of 4-5 % .

### 3.2 TIME RESOLUTION

When Ge(Li) detectors are applied for lifetime measurements by the delayed coincidence techniques, one can obtain a time resolution of the order of nanoseconds. However, the most important source of time spread is the dependence of the detector pulse rise time on the place of the interaction of gamma-rays inside the detector. For relatively high volume detectors (good detection efficiency), this effect will certainly deteriorate the time resolution of the system. However, in the present work the use of the constant fraction pulse height triggers largely compensate the effects of walk and rise time variation . In this work, the time resolution of the system was measured by performing delayed coincidences between the 1174 keV and the 1332 keV gamma lines populating and depopulating the 1332 keV level in  $^{60}\text{Co}$  source . The 1332 keV line was selected in the scintillation detector channel while the 1174 keV line was selected in the Ge(Li) detector channel. Fig.7-a shows the prompt resolution curve obtained when the 1332 keV line was detected by a 50 mm diameter x 50 mm high NaI(Tl) crystal. In this case, the time resolution curve obtained was found to have a full width at half maximum =  $2.61 \pm 0.1$  ns , a full width at tenth of the maximum =  $6.71 \pm 0.1$  ns while slopes of  $1.03 \pm 0.06$  and  $0.64 \pm 0.06$  ns for the two exponential decays of the prompt curve were obtained. When the 1332 keV line was detected by a 50 mm diameter x 50 mm high NE 102 plastic scintillator, the prompt resolution curve obtained (fig.7-b) was found to have a full width at half maximum =  $2.42 \pm 0.1$  ns , a full width at tenth of the maximum

$= 6.11 \pm 0.1$  ns, while the slopes of the two exponential decays of the prompt curve were found to be  $0.88 \pm 0.06$  and  $0.70 \pm 0.06$  ns.

#### 4. Lifetime of The 482 keV Level in $^{181}\text{Ta}$

The half-life of the 482 keV level in  $^{181}\text{Ta}$  has been measured by several authors using several techniques<sup>20-24</sup>). However, no measurements of the lifetime of such level using Ge(Li) detectors have been reported before. Therefore, we have found it useful to measure the half-life of this level using our Ge(Li) detector-scintillation detector timing system.

##### i) SOURCE PREPARATION

The excited levels of  $^{181}\text{Ta}$  is obtained from the decay of  $^{181}\text{Hf}$  to  $^{181}\text{Ta}$ . The  $^{181}\text{Hf}$  source was obtained by irradiating a sample of natural Hf oxide in the RAER at Inshass for a period of 48 hours at a neutron flux of the order of  $10^{12}$  n/cm<sup>2</sup>/s. Since natural hafnium contains a mixture of  $^{174}\text{Hf}$  (0.163%),  $^{176}\text{Hf}$  (5.21%),  $^{177}\text{Hf}$  (18.56%),  $^{178}\text{Hf}$  (27.1%),  $^{179}\text{Hf}$  (13.75%) and  $^{180}\text{Hf}$  (35.22%), the obtained activity only contained,  $^{175}\text{Hf}$  ( $T_{1/2} = 70$  days),  $^{180\text{m}}\text{Hf}$  ( $T_{1/2} = 5.5$  hours) and  $^{181}\text{Hf}$  ( $T_{1/2} = 42.5$  days). The source was used 20 days after irradiation and thus the main activity were due to  $^{175}\text{Hf}$  and  $^{181}\text{Hf}$  sources.

##### ii) MEASUREMENTS

Fig. 8 shows a partial decay scheme of the  $^{181}\text{Hf}$  nucleus<sup>26</sup>) in which only the most intense transitions are indicated.

In order to measure the lifetime of the 482 keV level in  $^{181}\text{Ta}$ , we have measured the single gamma-ray spectrum using both Ge(Li) detector and NaI(Tl) scintillation detector. According to the partial level scheme of  $^{181}\text{Ta}$  and the single gamma-ray spectra obtained, the lifetime of the 482 keV level in  $^{181}\text{Ta}$  was measured in two ways.

First, we performed delayed coincidences between the 133 keV

gamma-ray transition populating this level in the start channel (selected with the help of NaI(Tl) detector) and the 482 keV gamma-ray transition depopulating this level in the stop channel (selected with the help of Ge(Li) detector). The time spectrum thus obtained is given in figure-9 . The value obtained for the half-life of the 482 keV level in  $^{181}\text{Ta}$  is  $10.38 \pm 0.12$  ns . This value was deduced after the subtraction of the chance coincidences obtained with a prompt spectrum using  $^{22}\text{Na}$  source under the same experimental condition. The data were least-squares fitted .

Secondly, we have performed delayed coincidences between the 133 keV gamma-ray transition populating this level in the start channel (selected with the help of NaI(Tl) detector) and the 345 keV gamma-ray transitions depopulating this level in the stop channel (selected with the help of Ge(Li) detector). The time distribution spectrum obtained is given in fig. 10 . The prompt contribution observed in this spectrum was due to the presence (in the stop channel) of part of the 343.4 keV transition depopulating the fast 343.4 keV level in the  $^{175}\text{Hf} \rightarrow ^{175}\text{Lu}$  decay . In fact, this contribution could be reduced by choosing narrower window in the slow Ge(Li) detector channel. This solution was not used since narrower window will cause the elimination of part of the gamma-rays depopulating the 482 keV level under investigation and a reduction in the delayed coincidence counting rate will be obtained. From the obtained spectrum, the value deduced for the half-life of the 482 keV level in  $^{181}\text{Ta}$  is  $10.50 \pm 0.13$  ns. This value was deduced by least-squares fitting after the subtraction of the chance coincidences obtained with the prompt spectrum of a  $^{22}\text{Na}$  source, under the same energy settings.

From the results obtained from these two measurements, no significant differences in the values of the measured half-lives are noticed .

Taking into consideration the statistical and systematic errors due to time calibration and electronic instability of the apparatus, a mean value for the half-life of the 482 keV level deduced from the slopes of the time distribution curves was found to be ,

$$T_{\frac{1}{2}} (482 \text{ keV level}) = 10.49 \pm 0.09 \text{ ns}$$

### 5. Discussion

The investigation done in this work have permitted us to study in details the characteristics and performance of the described system. Such study is very useful in order to obtain the best operating conditions as well as the maximum capabilities of the system. The system described here can be used to measure accurately gamma-ray energies with a resolution ranging from  $\approx 1$  keV at gamma-ray energy of the order of 100 keV to a resolution  $\approx 2$  keV at gamma-ray energy of the order of 1 MeV. In addition the relative gamma transitions could be also obtained in the energy range from  $\approx 60$  to  $\approx 2400$  keV. However, below  $\approx 200$  keV the detection efficiency decreases rapidly due to the absorption of gamma radiations in the dead layer of the detector and in its packing materials. Concerning the time resolution of the system, the prompt resolution curves obtained showed that lifetimes in the nano-second range could be easily measured by relatively large volume Ge(Li) detectors. In addition, the value of the half-life of the 482 keV level in  $^{181}\text{Ta}$  nucleus obtained in this work  $10.49 \pm 0.09$  ns is in excellent agreement with the most recent value  $(10.81 \pm 0.05)$  ns obtained by Lowe et al. <sup>24)</sup> in 1973 and with the values  $(10.56 \pm 0.15)$ ,  $(10.40 \pm 0.2)$ ,  $(11.0 \pm 0.2)$  ns and  $(11.02 \pm 0.35)$  ns reported by references 20, 23 respectively. However, using the theoretical values of the internal conversion coefficients tabulated by Sliv and Band <sup>25)</sup> and the branching ratios of the different gamma-ray lines depopulating this level,

the experimental partial gamma-ray half lives  $T_{\frac{1}{2}\text{exp}}$  for all transitions have been calculated using the formula ,

$$T_{\frac{1}{2}\text{exp}} = \frac{T_{\frac{1}{2}\text{obs.}} (1 + \alpha)}{\alpha}$$

These values are compared with the theoretical single particle Weisskopf estimates<sup>16)</sup> given by ,

$$T_{\frac{1}{2}W} (M1) = 2.24 E_{\gamma}^{-3} 10^{-5} \text{ ns ,}$$

$$T_{\frac{1}{2}W} (E2) = 9.37 A^{-4/3} E_{\gamma}^{-5} \text{ ns and}$$

$$T_{\frac{1}{2}W} (M2) = 11.9 A^{-2/3} E_{\gamma}^{-5} \text{ ns.}$$

where  $E_{\gamma}$  is the gamma-ray transition energy in MeV.

To obtain the Weisskopf estimate a nuclear radius constant of 1.2 fm and a statistical factor  $S = 1$  were used<sup>16)</sup>.

Table 1 shows the hindrance factors calculated relative to the theoretical single-particle Weisskopf estimate of the partial half-lives. The retardation factors for the 482 keV and the 345 keV E2 transitions are similar. It is difficult to understand why the 482 keV M1 transition is more than  $10^3$  times more retarded than is the other 476 keV M2 transition.

Table 1

Hindrance factor for gamma-ray transitions of the 482 keV level in  $^{181}\text{Ta}$  nucleus

$E_{\gamma}$ transition (KeV)	Multipolarity	$T_{\frac{1}{2}\gamma}^{\text{exp}}$ (ns)	$T_{\frac{1}{2}\gamma}^{\text{exp}} / T_{\frac{1}{2}W}$
482	E 2	12.80	36.57
	2 % M 1	13.25	$6.62 \times 10^4$
476	pure M2	624.60	16.02
345	pure E2	77.39	42.99

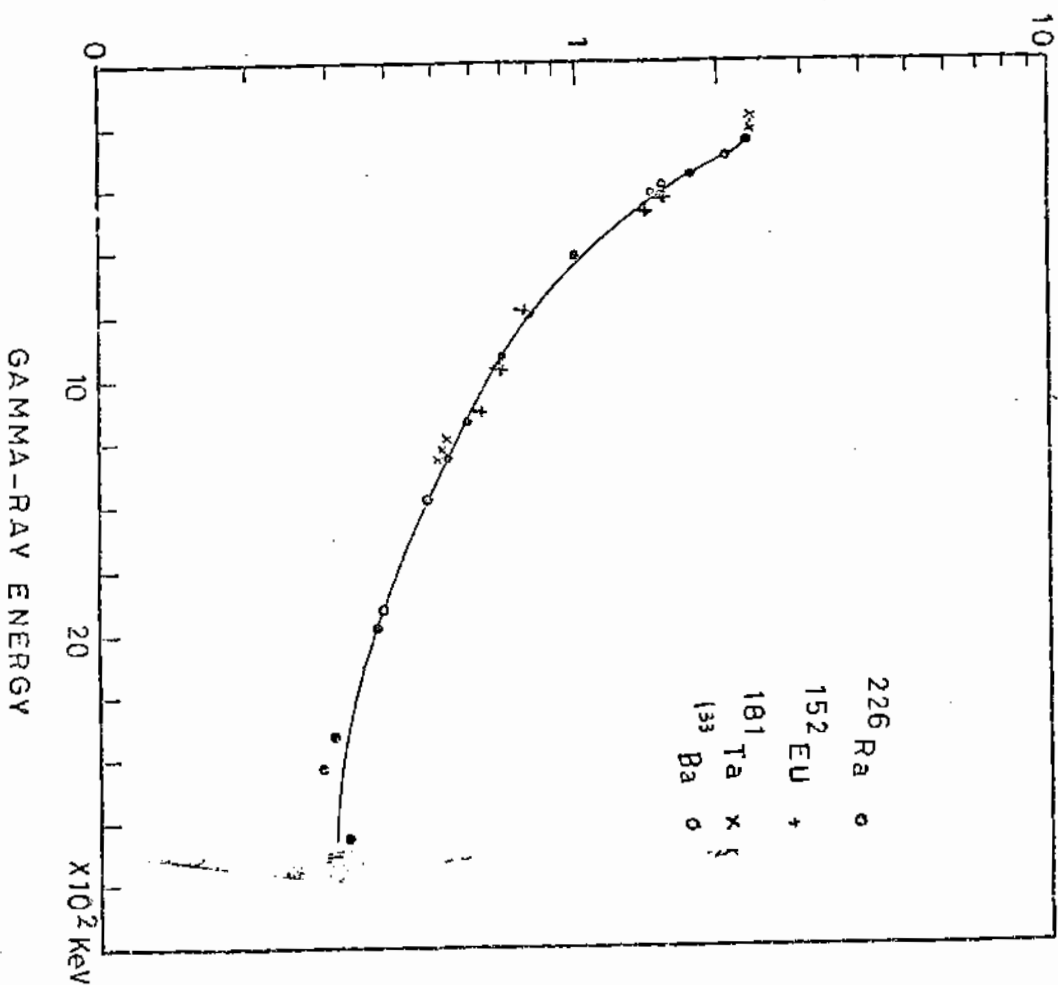
\* From our present work.

References

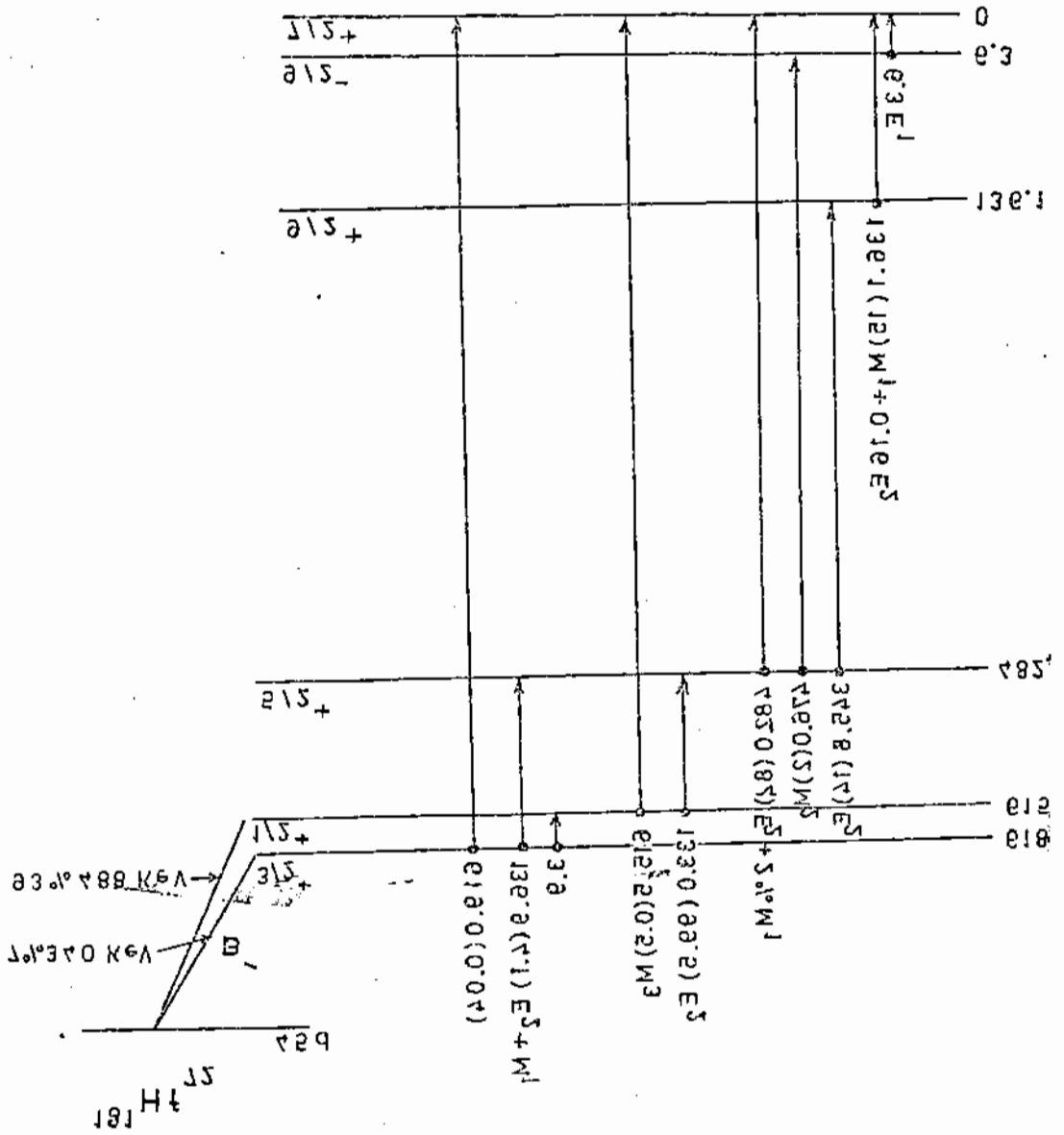
1. M. Moszynski and B. Bengtson, Nucl. Instr.&Meth. 80(1970)233
2. Z. H. Cho and J. Llacer, Nucl. Instr. & Meth. 98(1972)461
3. B. Bengtson and M. Moszynski, Nucl. Instr. Methods 100(1972)293
4. F. Gabriel, H. Koepernik and K. Schops, Nucl. Instr. Methods 103(1972)501
5. L. Karlsson, Nucl. Instr. Methods 106(1973)161
6. P. G. Coulter, H. C. Evans and B. C. Robertson, Nucl. Instr. Methods 117(1974)259
7. D. C. S. White and W. J. McDonald, Nucl. Instr. Methods 115(1974)1
8. J. Kozyczkowski and J. Bialkowski, Nucl. Instr. Methods 137(1976)75
9. J. C. Balland, J. Pigneret, J. J. Samueli and A. Sarazin, IEEE Trans. Nucl. Sci. NS-15, no. 1(1968)411
10. R. Stuck, J. A. Mische, E. Ostertag, R. Henok and P. Siffert, Proc. Nucl. Electron Symp. (Versailles, Sept. 1968)
11. M. Cocchi, A. Rota, M. Jacquin and J. C. Balfand, Proc. Nucl. Electron Symp. (Versailles, Sept. 1968)
12. J. C. Balland, M. Goyot, J. Guyon, J. Pigneret, J. J. Samueli and A. Sarazin, Proc. Nucl. Electron Symp. (Versailles, Sept. 1968)
13. G. Haouat, J. Lachkar and J. Signaud, Proc. Nucl. Electron Symp. (Versailles, Sept. 1968)
14. H. Abou-Leila, A. A. El Kamhawy, H. A. Ismail, S. M. Darwish, A. Ibrahim, Bulletin of Bin Shams University College for Girls, to be published
15. H. Abou-Leila, A. A. El Kamhawy, H. Hanafy, S. M. Darwish, H. A. Ismail and S. Abd El Malak, to be published
16. S. A. Moszkowski, alpha-, beta-, and gamma-spectroscopy ed. by K. Siegbahn (N. H. Publ. Co., Amsterdam 1965) p. 881
17. U. Fano, Phys. Rev. 72 (1947) 26
18. P. M. Grant, Nucl. Instr. Methods 127(1975)371
19. H. Abou-Leila, H. A. Ismail, S. M. Darwish, M. Kamel and A. El Ashry, to be published
20. T. D. Nainon, Phys. Rev. 123(1961)1751

21. R. W. Somerfeldt, T. W. Gannon, L. W. Goleman and L. Schecter,  
Phys. Rev. 138(1965)B763
22. W. Meiling and F. Stary, Nucl. Phys. 74(1965)113
23. P. D. Bond, J. D. McGervey and S. Jha, Nucl. Phys. A163(1971)571
24. L. M. Lowe, H. Zmora and W. V. Prestwich, Can. J. Phys. 51(1973)1497
25. L. A. Sliv and J. M. Band, alpha-,beta- and gamma-spectroscopy ed.  
by K. Siegbahn (N. H. Publ. Co., Amsterdam, 1965)p.881
26. C. M. Lederer, J. M. Hollander and I. Perlman, Table of Isotopes  
(John Wiley & Sons , N. Y., 1968)

# RELATIVE EFFICIENCY



181 19 13



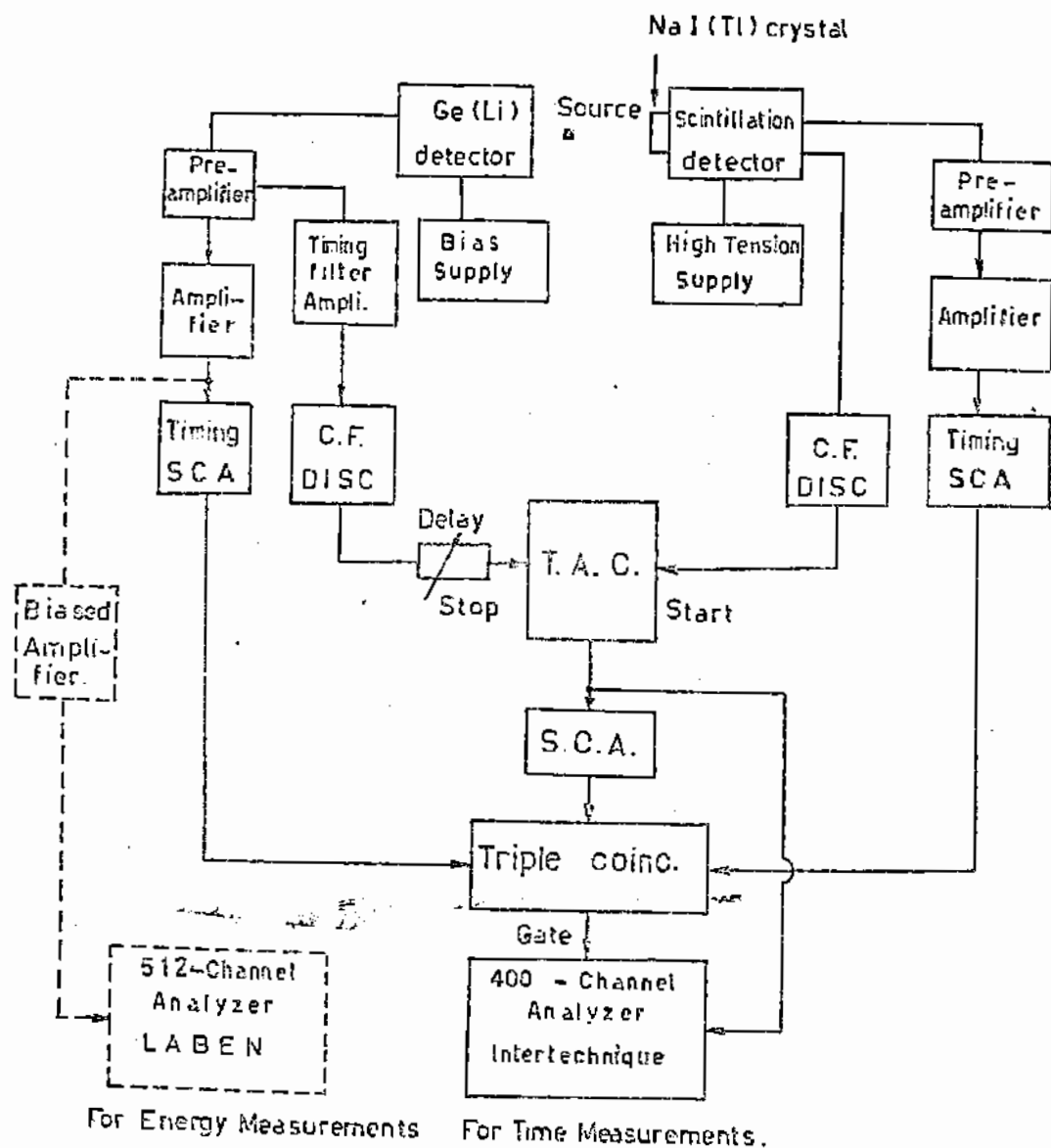


Fig. 1

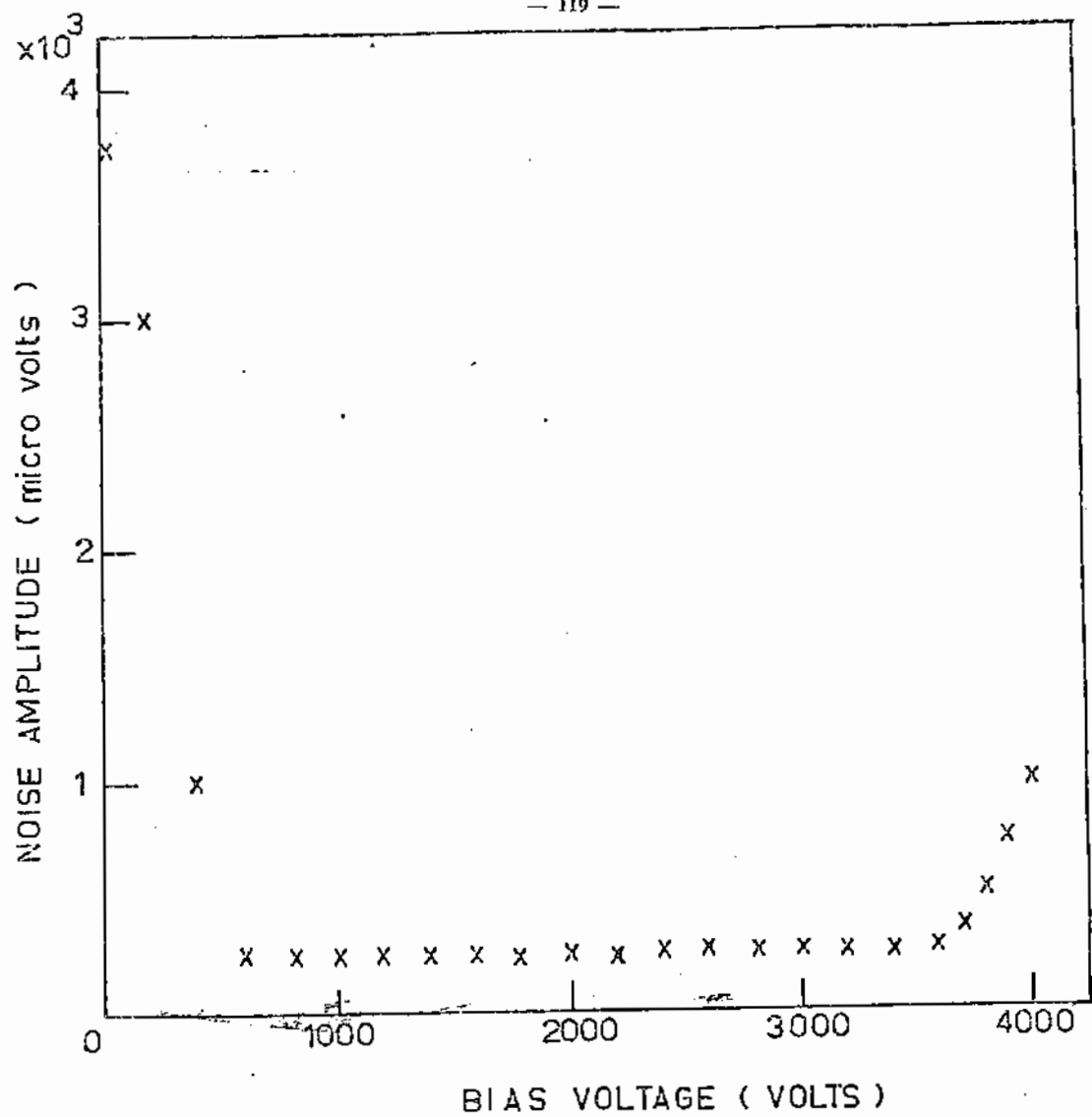
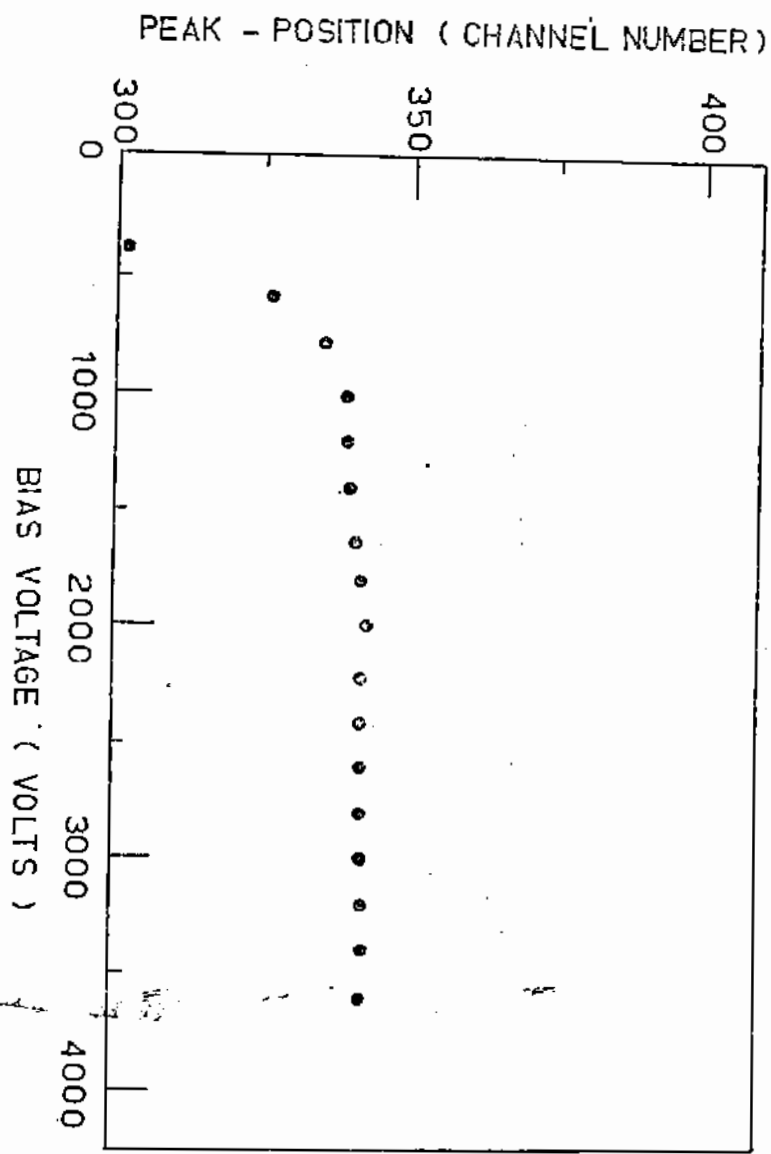


Fig. 2c



— 120 —

Fig. 2 (B)

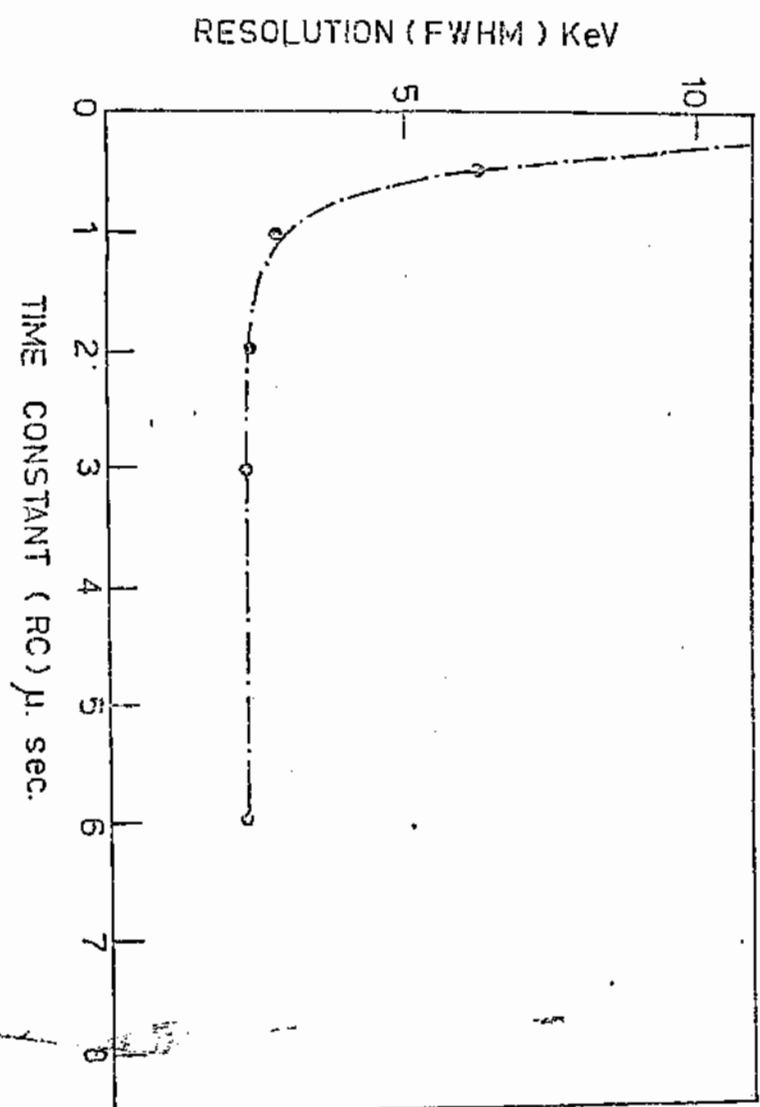
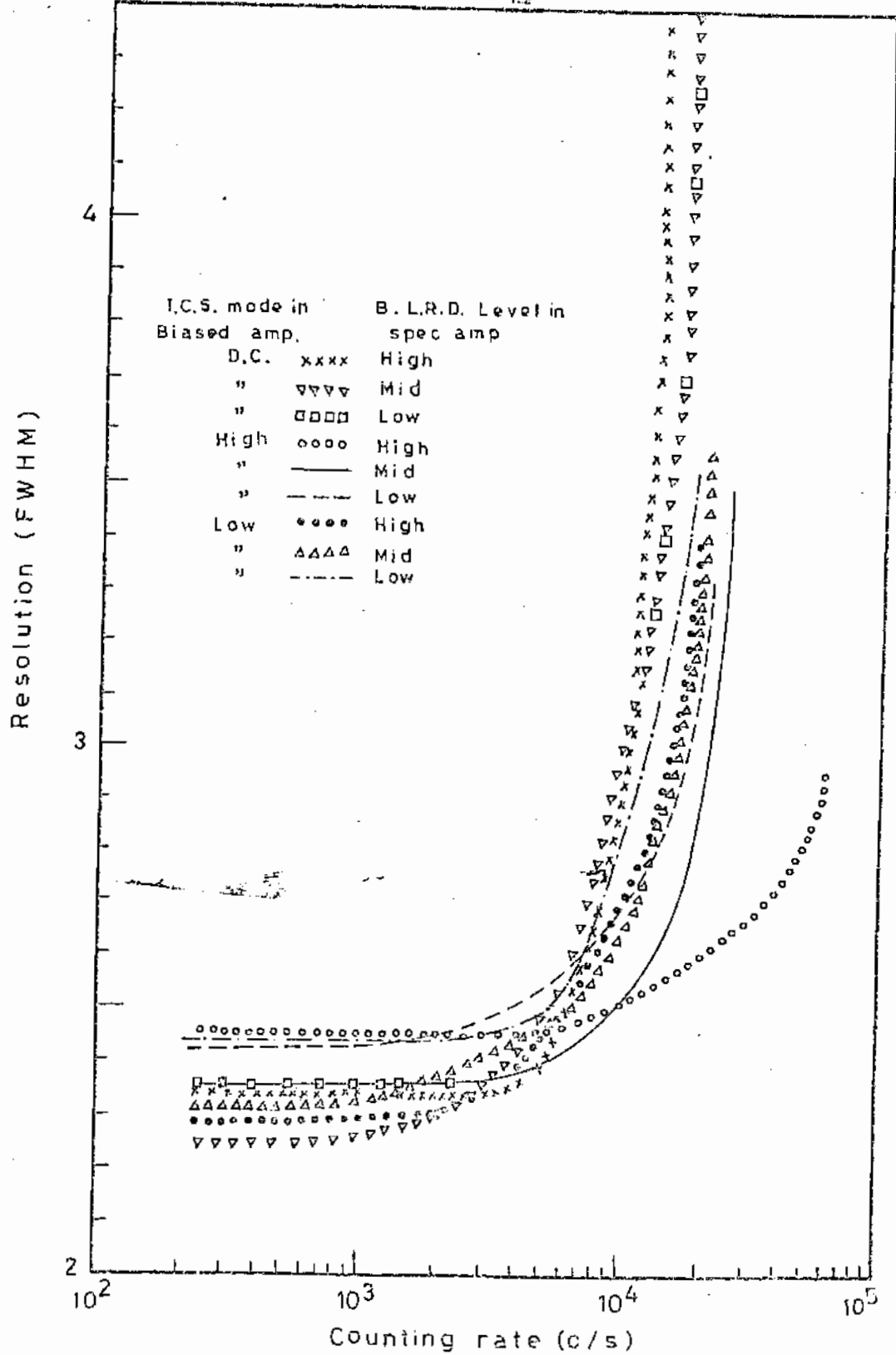
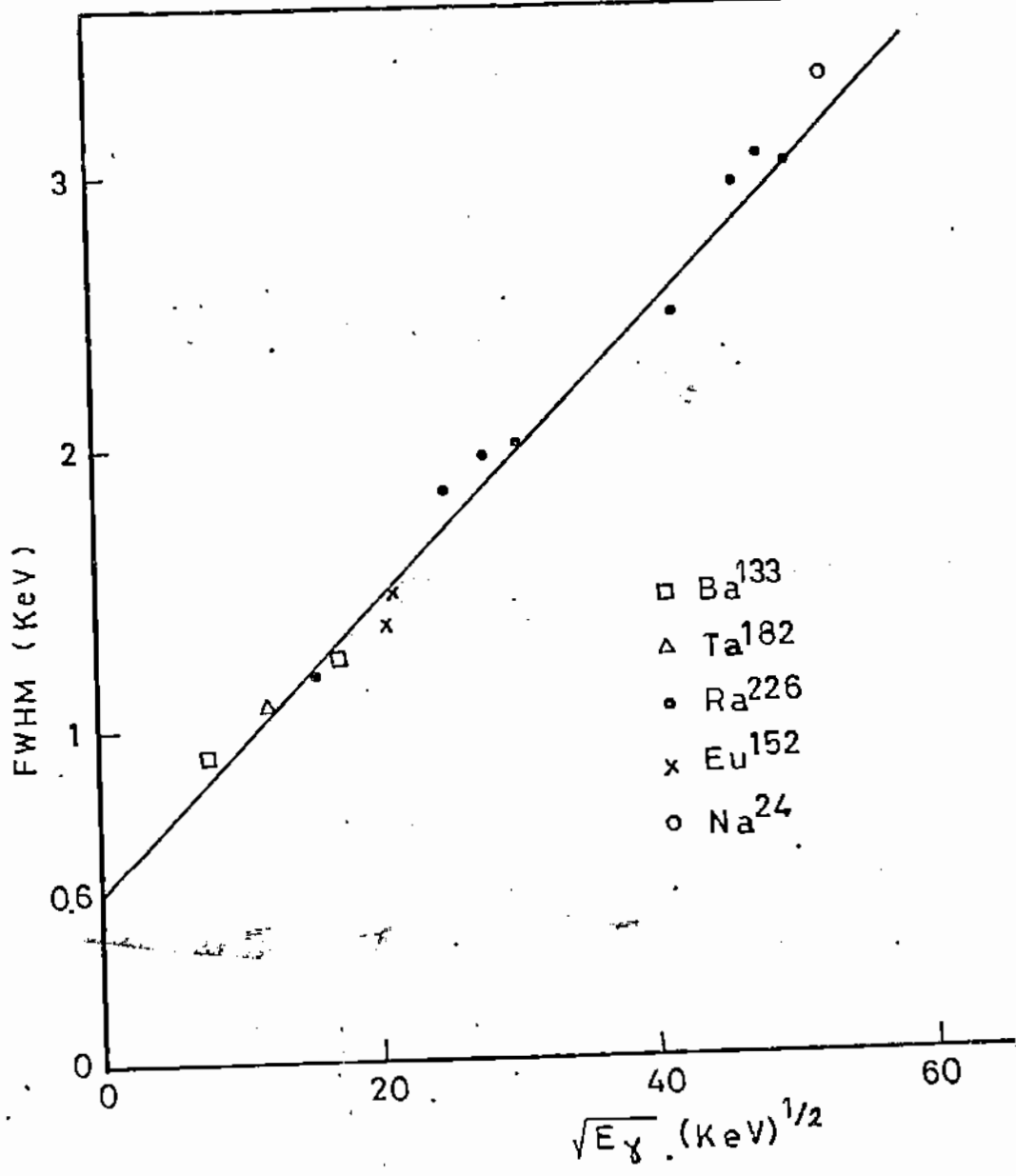


Fig. 3





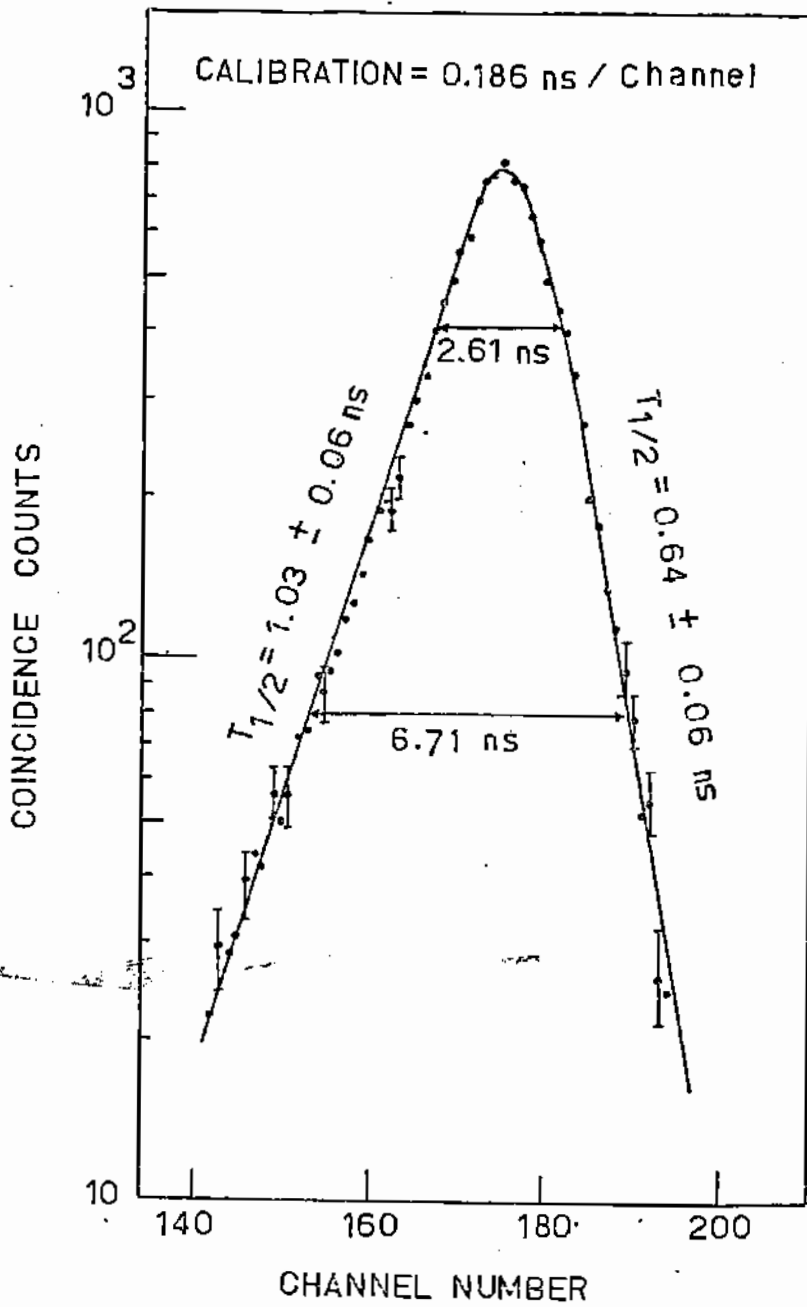


Fig. 7(a)

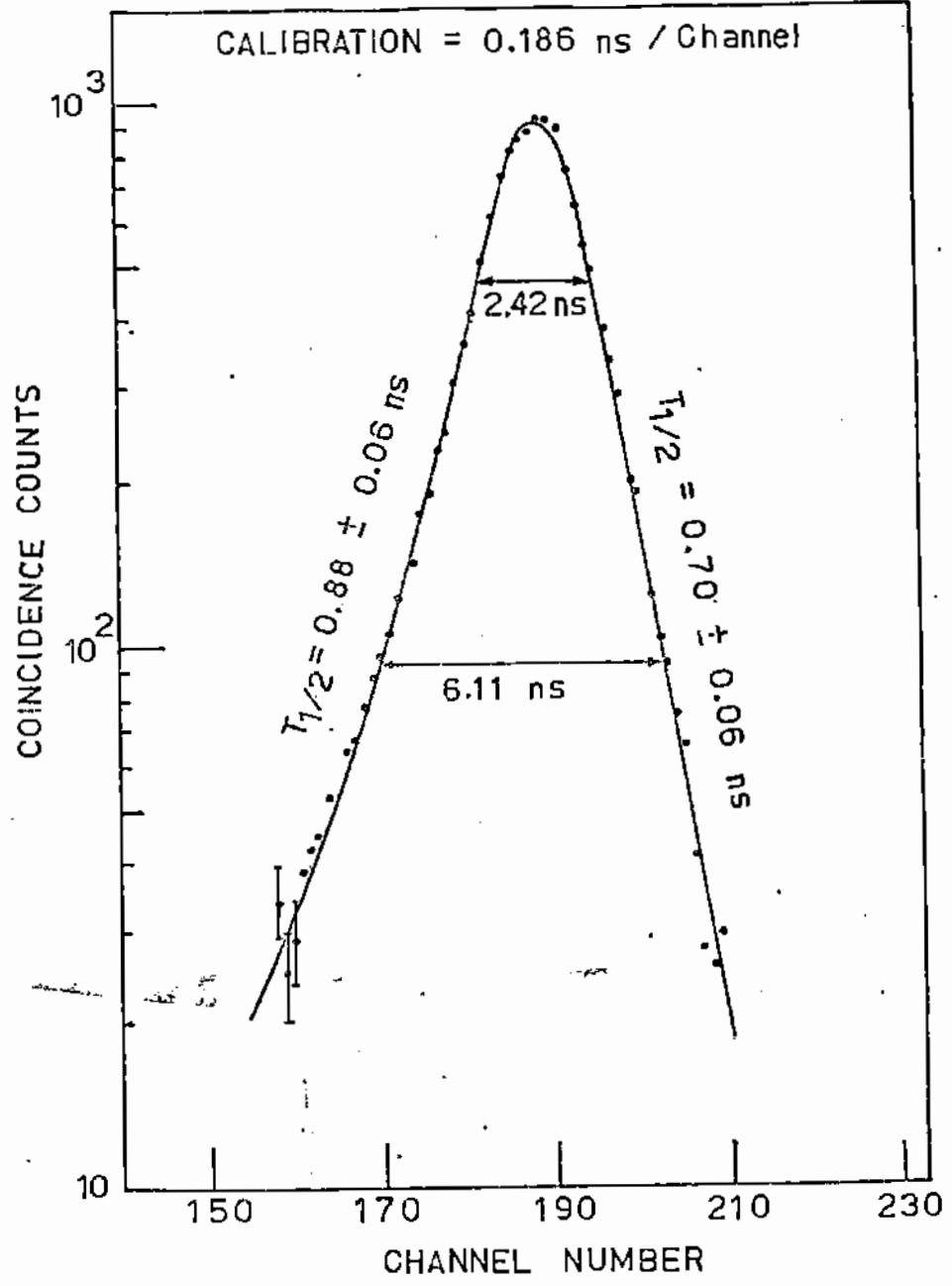


Fig. 7

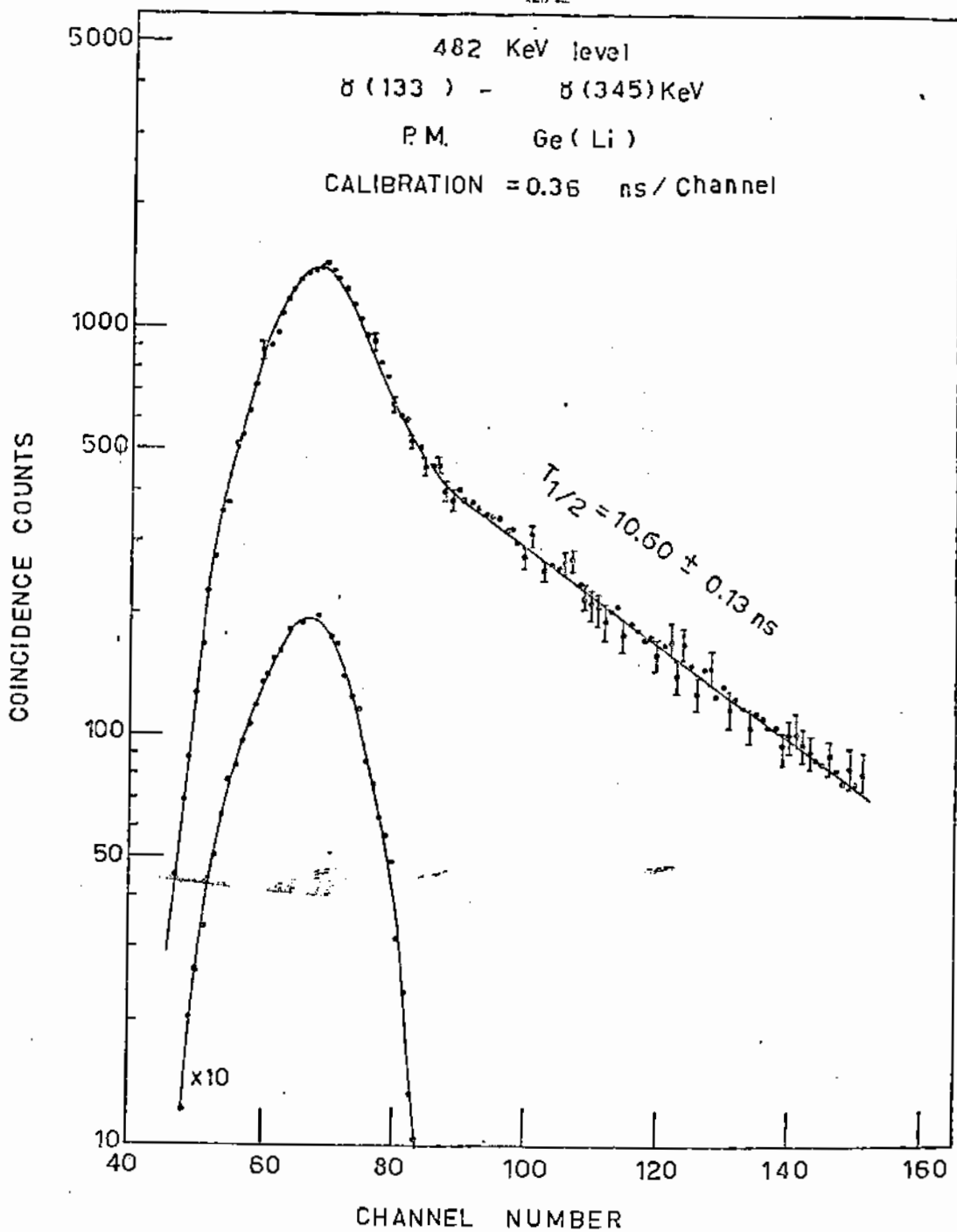


Fig. 3

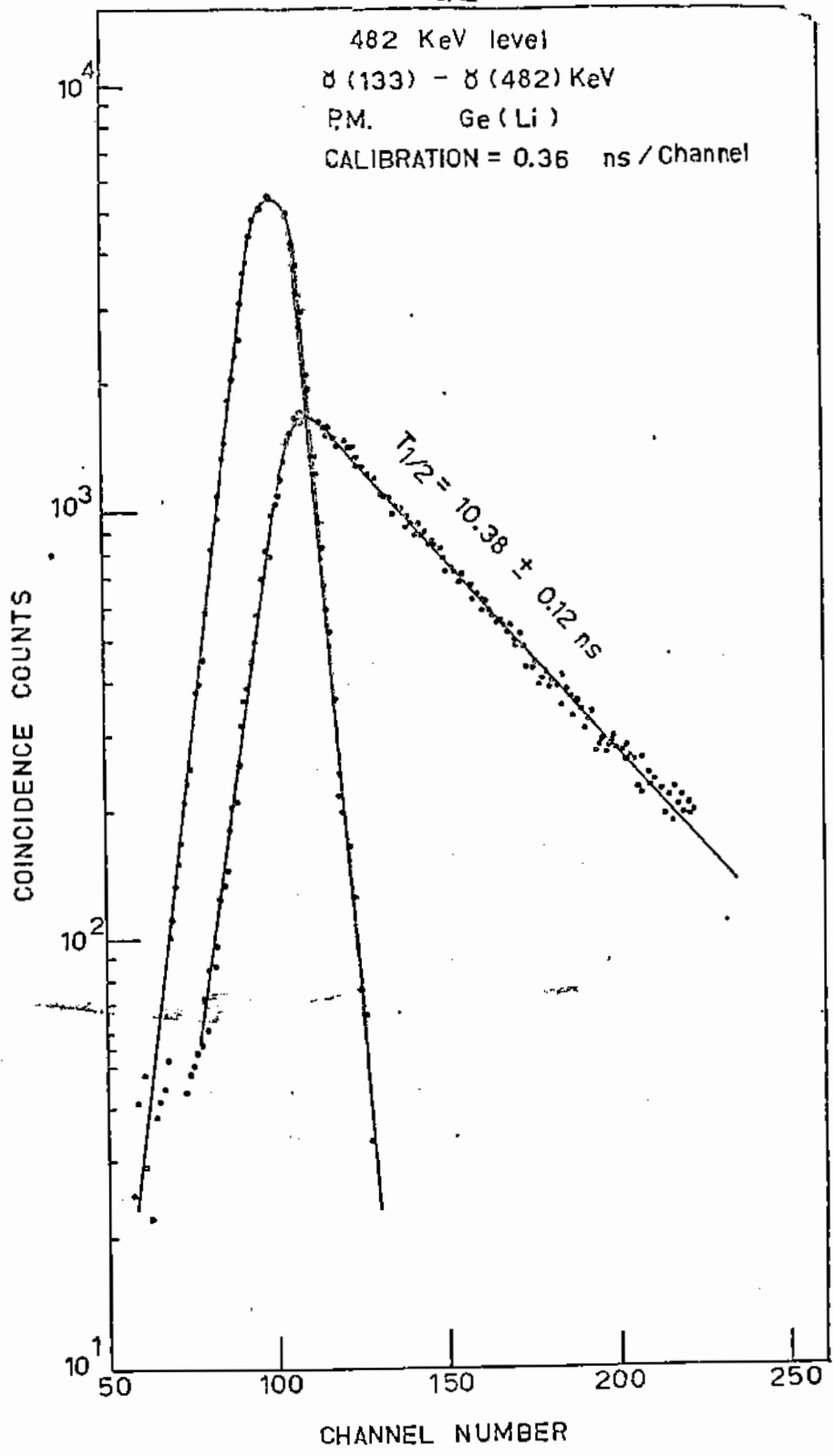


Fig. 8

Figure Captions

- Fig. 1 : Block diagram of the system.
- Fig. 2 a) The dependence of the detector noise (pre-amplifier output) on the applied bias at different bias voltages.
- b) The effect of the detector bias on the detector pulse height output using a  $^{137}\text{Cs}$  source.
- Fig. 3 : Gamma-ray energy resolution of the Ge (Li) spectrometer as a function of amplifier shaping time constant
- Fig. 4 : Effect of input circuit selection (I.C.S.) mode in spectroscopy amplifier and base line restoration discriminator level (B.L.R.D.) in biased amplifier on energy resolution.
- Fig. 5 : Linear variations of the spectrometer energy resolution with the square root of the gamma-ray energy.
- Fig. 6 : Relative photo peak efficiency for different gamma-ray energies of the Ge (Li) detector.
- Fig. 7 : Prompt time resolution curve for the 1332 keV level of  $^{60}\text{Co}$ .
- a) detected by 50 mm dia x 50 mm high NaI (Tl) scintillation detector in the start channel and Ge(Li) detector in the stop channel,
- b) detected by 50 mm dia x 50 mm height NE 102 plastic scintillation detector in the start <sup>channel</sup> and a Ge(Li) detector in the stop channel.
- Fig. 8 : A partial decay scheme of the  $^{181}\text{Hf}$  nucleus (Ref. 26).
- Fig. 9 : Delayed time distribution coincidence spectrum for the 482 keV level in  $^{181}\text{Ta}$ , (133 keV) gamma-ray line in the start channel and (482 keV) gamma-ray line in the stop channel.
- Fig. 10 : Delayed time distribution coincidence spectrum for the 482 keV in  $^{181}\text{Ta}$  (133 keV) gamma-ray line in the start channel and (345 keV) gamma-ray line in the stop channel.